

Imaging of Temperature Distribution and Retinal Tissue Changes during Photocoagulation by High Speed OCT

Heike H. Müller^a, Lars Ptaszynski^a, Kerstin Schlott^a, Tim Bonin^a, Marco Bever^a, Stefan Koinzer^c, Reginald Birngruber^{a,b}, Ralf Brinkmann^{a,b}, and Gereon Hüttmann^{a,b}

^aInstitute of Biomedical Optics, University of Lübeck, Peter-Monnik-Weg 4, Lübeck, Germany*;

^bMedical Laser Center Lübeck GmbH, Peter-Monnik-Weg 4, Lübeck, Germany;

^cClinic of Ophthalmology, Arnold-Heller-Straße 31, Kiel, Germany

ABSTRACT

Considerable improvement in the reproducibility of retinal photocoagulation is expected if degree and extend of the heat-induced tissue damage can be visualized on-line during the treatment. Experimental laser treatments of the retina with enucleated pig eyes were investigated by high speed phase-sensitive OCT. OCT could visualize the increase of tissue scattering during the photocoagulation in a time-resolved way. Immediate and late tissue changes were visualized with more than 15 μm resolution. Changes of the reflectance in the OCT images had a similar sensitivity in detecting tissue changes than macroscopic imaging. By using Doppler OCT slight movements of the tissue in the irradiated spot were detected. At low irradiance the thermal expansion of the tissue is observed. At higher irradiance irreversible tissue changes dominate the tissue expansion. OCT may play an important role in understanding the mechanisms of photocoagulation. This may lead to new treatment strategies. First experiments with rabbits demonstrate the feasibility of in-vivo measurements.

Keywords: Optical coherence tomography, Doppler OCT, photocoagulation, sub-threshold, tissue effects

1. INTRODUCTION

Photocoagulation is one of the most successful laser therapies in medicine. By irradiating the retina with a cw-laser, tissue damage is produced, which spans from the retinal pigment epithelium (RPE) to the adjacent parts of the neural retina. Recently, an interest in more selective retinal treatments is observed. With microsecond irradiation or near threshold coagulation, a damage confined to the RPE is possible.¹⁻³ Clinical success of these low damage therapy concepts depend crucially on the ability to choose the irradiation parameter individually. The selective retina therapy (SRT) which relies on the formation of cavitation bubble for cell destruction uses an acoustic detection of the bubble formation for dosimetry.^{4,5} Recently a non-invasive measurement of the temperature rise during conventional photocoagulation was developed which uses a few degree temperature jump by an additional nanosecond pulsed laser to generate an optoacoustic signal.⁶ A sensitive microphone which is integrated in a contact glass measures the strength of the acoustic transient which correlates with the background temperature on which the nanosecond temperature increase is produced.⁷ Other proposed approaches for dosimetry of photocoagulation include measurement of light scattering or autofluorescence during the irradiation. However, all methods which were proposed so far provide no spatial resolution and can not directly show the effect of the irradiation on the different retinal layers.

*Further author information: (Send correspondence to G.H..)

H.H.M.: E-mail: Mueller@bmo.uni-luebeck.de, Telephone: +49 (0) 451 500 6509

L.P.: E-mail: Ptaszynski@bmo.uni-luebeck.de, Telephone: +49 (0) 451 500 6516

K.S.: E-mail: Schlott@bmo.uni-luebeck.de, Telephone: +49 (0) 451 500 6517

T.B.: E-mail: Bonin@bmo.uni-luebeck.de, Telephone: +49 (0) 451 500 6510

M.B.: E-mail: Bever@bmo.uni-luebeck.de, Telephone: +49 (0) 451 500 6521

S.K.: E-mail: koinzer@auge.uni-kiel.de, Telephone: +49 (0) 431 597 4834

R.B.: E-mail: Bgb@bmo.uni-luebeck.de, Telephone: +49 (0) 451 500 6504

Ra.Br.: E-mail: Brinkmann@bmo.uni-luebeck.de, Telephone: +49 (0) 451 500 6507

G.H.: E-mail: Huettmann@bmo.uni-luebeck.de, Telephone: +49 (0) 451 500 6530

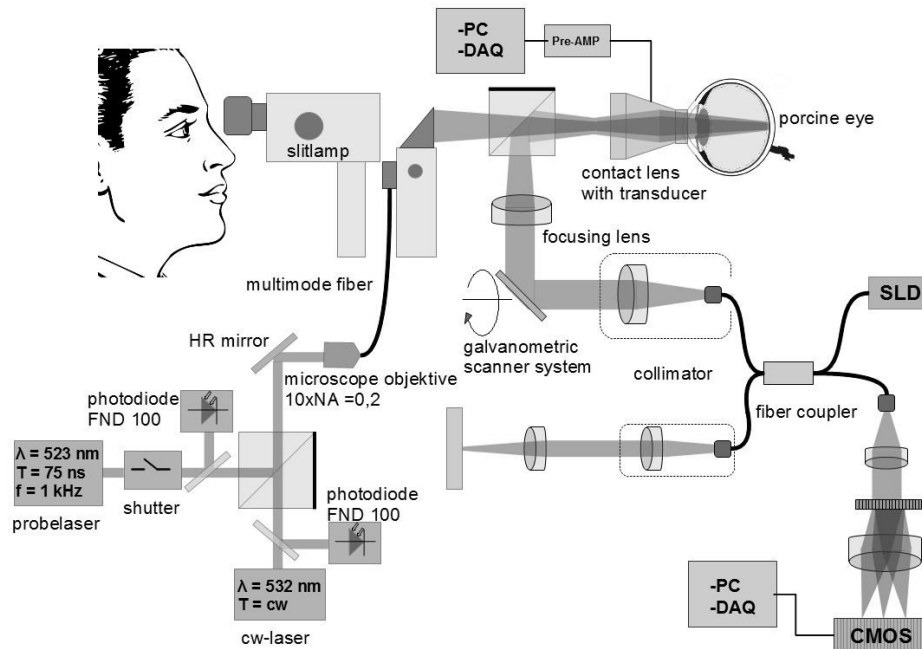


Figure 1. Optical setup for simultaneous measurements of temperature and OCT during photocoagulation. All laser are coupled via a slit-lamp and several beam splitters into the eye. The high speed OCT consists of a spectrometer, an open interferometer and a 2-axis galvanometric scanner.

OCT is the only non-invasive imaging modality, which can visualize the layered structure of the retina in-vivo. Though post-operatively OCT images showed changes of tissue morphology due to the photocoagulation,⁸ the direct response of the tissue during and shortly after irradiation was not yet investigated by OCT and is essentially not known. OCT imaging during the photocoagulation is principally feasible and may play an important role in understanding the mechanisms of photocoagulation. The high sensitivity of OCT to movements can be used to measure slight dynamic tissue changes during coagulation.⁹ It may lead to a new dosimetry or treatment strategies for photocoagulation.

Aim of this study was to visualize the tissue changes in the pig and rabbit retina during photocoagulation by high speed phase sensitive OCT. Experimental laser irradiation of the retina of enucleated porcine eyes was followed by high speed phase-sensitive OCT, which visualized the increase of tissue scattering and tissue movements during the photocoagulation in a time-resolved way. The measured OCT images were correlated with fundus images and measurements of the temperature increase during the coagulation by a new optoacoustic thermometer. First experiments in anesthetized rabbits are also presented.

2. MATERIAL AND METHODS

2.1 Experimental Set Up

For OCT measurements during photocoagulation a high speed OCT (Hyperion, Thorlabs-HL AG, Lübeck, Germany) at a wavelength of 840 nm was interfaced with a cw coagulation laser (wavelength 532 nm) and a pulsed laser (wavelength 523 nm) for the optoacoustic temperature measurements (see Fig. 1). All three beams were combined by beam splitters and focused through a contact glass which also contained the acoustic transducer for the registration of the pressure transients. The system for optoacoustic measurements consists of the probe laser and the microphone in the contact glass with amplifier and PC. The laser emitted 75 ns pulses with an energy of 7 μJ at 1 kHz repetition rate. A ring shaped piezo transducer in the contact glass measured the pressure transients caused by the nanosecond probe pulses. If the temperature in the probe volume increased, the optoacoustic transients also increased because of the temperature dependence of the Grüneisen parameter of

the tissue.¹⁰ With a calibration, which was made by continuous heating with direct temperature measurement, the relative optoacoustic signal increase was converted to a temperature increase.

By using test lesion and volumetric scans it was possible to place the treatment beam, the optoacoustic probe beam, and the OCT beam on one common axis. OCT images (250 A-scans per B-scans) were continuously recorded with 200,000 A-Scans/s from a region in and around the coagulation spot, starting before the coagulation until a few hundred milliseconds after the tissue exposure. Series of coagulations with increasing laser power (10 mW to 140 mW on the cornea) were investigated for different exposure times (10 ms to 1 s) and spot sizes (50 μm to 200 μm). The enucleated pig eyes were obtained from the local slaughter house and used within 6 hours. A special fixation stage was used by which the custom designed contact glass with a piezo ring transducer was fixed to eye. Both were firmly attached to the slit-lamp, which delivered the OCT.

First in-vivo experiments were conducted with 3 rabbits, which were anesthetized during the experiment. The animals were hold by a special fixation state which stood on the same optical table as the slit-lamp. Animal experiments were approved by the Government of Schleswig-Holstein under application V312-72241.121-11 (10-2/09).

2.2 Data Evaluation

The spectra measured by the Hyperion OCT were streamed during the irradiation to a hard disk drive and the calculation of the A-scans was done off-line. After correction of background, spectral shape and resampling to a linear k-scale the measured spectra were Fourier transformed to obtain the complex A-scans. The absolute value of the A-scans was displayed on a logarithmic scale as the scattering intensity. To see small tissue changes also the phase of the A-scans was analyzed. Since the phase changes between adjacent A-scans was too small, we subtracted the phase at each pixel from two following B-scans, which were separated by $\Delta t = 1.3$ ms in time. From the phase difference $\Delta\varphi$ of the two images the velocity v_z , by which the tissue was moving parallel to the OCT beam (i.e. the z-direction) was calculated:

$$v_z(t) = \frac{\lambda_0}{4\pi n} \frac{\Delta\varphi}{\Delta t} \quad (1)$$

The center wavelength in air and the refractive index of the tissue are given here by λ_0 and n , respectively. By integration of the calculated velocity over the time course of the laser irradiation the actual displacement of the tissue $\Delta z(t)$ was calculated:

$$\Delta z(t) = \int_0^t v_z(\tau) d\tau \quad (2)$$

The local displacement was then averaged over the irradiated spot and compared to the optoacoustically measured temperatures.

3. RESULTS AND DISCUSSION

Series of laser exposures with decreasing radiant were applied to the retina of the enucleated eyes. Their appearance was documented by fundus images (Fig. 2). Similar to the in-vivo situation, a whitening of the irradiation lesions was observed which decreased in intensity and size as the irradiance was reduced. The measured peak temperature increases ranged from 0 K to over 50 K. In the OCT images the increased scattering of the lesions was seen as an increase of the reflectivity which builds up during the irradiation of the retina. This is demonstrated in Fig. 3, which shows three representative irradiation spots, one invisible, one slightly visible, and one strongly visible lesion, which were obtained at at 77 W/cm², 190 W/cm², and 410 W/cm², respectively. In the invisible lesions no increase in scattering was observed in the OCT images during and after irradiation. Only some fluctuation of the speckle patterns were seen. In the slightly visible lesions the scattering increased at the end of the irradiation just above the RPE layer. In the visible lesions, the hyperreflectivity started during the irradiation in the center of the coagulation spot just above the RPE and progressed laterally as well as upwards into the neural layer. The upper parts of the retina itself seemed not to be affected. For a radiant power, which

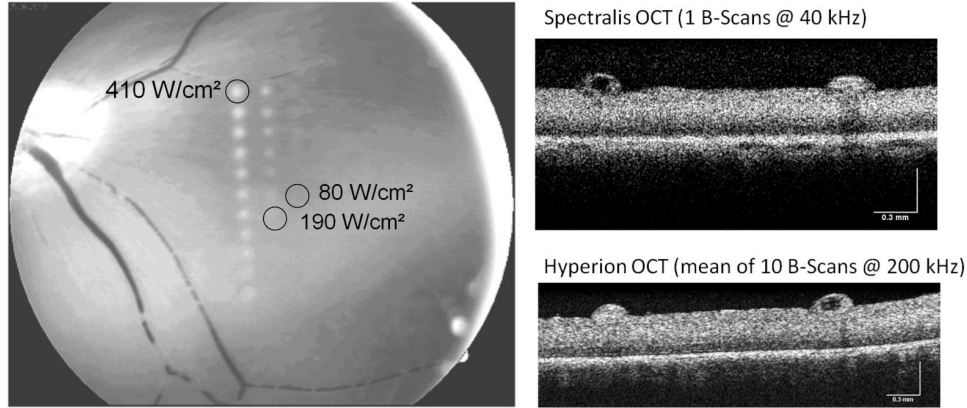


Figure 2. Retinal image of an enucleated pig eye after application of 31 laser coagulations with radiant power decreasing from 130 mW to 5 mW. Spot size was 200 μm , exposure time 400 ms. The three marked spots are examples for a strong lesion, a medium lesion, and a soft lesion, for which OCT images are presented later. On the right side a comparison of the image quality of our high speed OCT with an Heidelberg Engineering Spectralis is shown. After enucleating the pig eyes the retina of loses almost all of its structure.

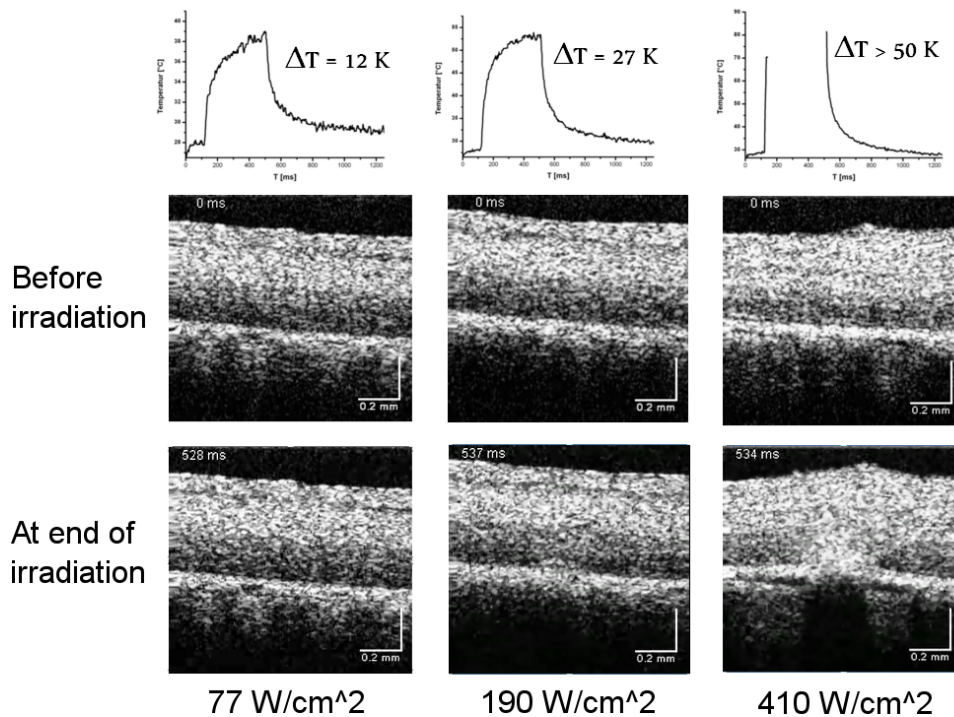


Figure 3. OCT images and temperature vs. time curve from three exposures of the retina with 77 W/cm^2 , 190 W/cm^2 , and 410 W/cm^2 , respectively. OCT intensity images before the beginning and at the end of the irradiation are shown.

produced strong lesions, elevated scattering started earlier during the laser exposure and progressed from the RPE to higher layers. In addition, massive distortions of the whole retina were seen (see Fig. 3). The dynamic tissue changes continued even after the end of the irradiation.

The speckle fluctuations during the subthreshold irradiation indicated some tissue movement may have been caused by the irradiation. Therefore Doppler images we calculate from phase difference between neighbored B-Scans with a time difference of 1.2 ms. The calculated phase differences are more sensitive to the movement of tissue than the speckle movements. A clear translation of the irradiated volume above the RPE in the direction of the OCT beam was visible, which was maximal when the laser was switched on. When the laser was switched

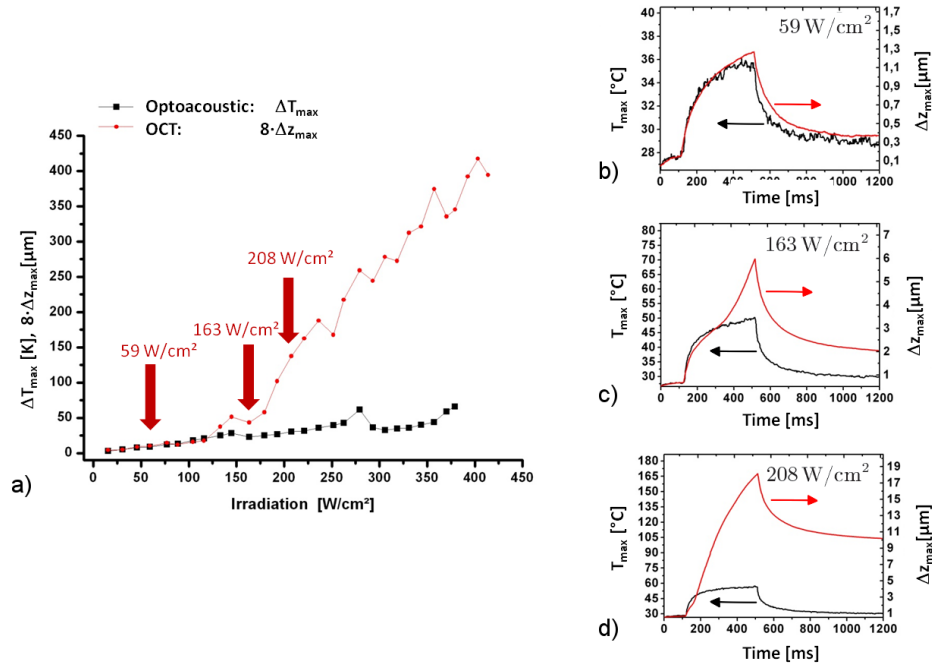


Figure 4. Correlation between the expansion Δz of the irradiated volume as well as the optoacoustically measured temperature with the irradiance. Peak expansion Δz_{max} and peak temperature ΔT_{max} was calculated and plotted versus the irradiance (a). For 59 W/cm^2 time course of expansion Δz follows temperature increase ΔT (b). At 163 W/cm^2 Δz suddenly shows a nearly twice increase compared to ΔT and does not return to the original level (c). With an irradiance of 208 W/cm^2 both curves look quite different (d).

of a reverse movement (i. e. a contraction) was observed.

By integration of the phase signal according to Eq. 2, the total time course of expansion and contraction was calculated (Fig. 4). For an irradiance below 120 W/cm^2 a linear relationship between the peak temperature ΔT_{max} as well as the peak expansion Δz_{max} , which both occurred at the end of the laser heating, and the irradiance were found. In this regime also the time traces of expansion and temperature match quite well (Fig. 4b). We assume that here the OCT measures the a reversible thermal expansion of the tissue. Hence OCT may be an alternative option for non-invasive temperature measurements during laser heating of tissue.

At higher irradiance the peak expansion starts to increases with a higher slope than the peak temperature and also the time courses start to differ at a certain point in time (Fig. 4c). In addition the expansion does not go back to its original value. The additional irreversible component seems to be associated with thermal denaturation of the tissue. As expected for thermal tissue damage, the superlinear behavior sets in earlier and the non-reversal component increased for higher temperatures (Fig. 4d). Even in the nonvisible lesions, where no changes in the B-Scan image were visible, a deviation of the expansion for a linear thermal expansion was observed, which may allow to identify for the physician not visible subthreshold lesions.

In vivo, additional movements due to heart beat, breathing or vibrations of the animal fixing stage contribute to the Doppler signal. In our preliminary animal experiments we observed that they contribute significantly to the OCT phase signal and obscured thermally induces tissue movement. However, these movements are bulk movements which affect the whole field of view in a similar way. Therefore we developed a simple algorithm, which calculates over a certain depth the average phase as a function of the lateral direction (Fig. 5a). To this curve a linear correction function is fitted and subtracted from the original data. With these simple motion correction algorithm it was possible to get first measurements of tissue movements during photocoagulation in vivo (Fig. 5b). At lower irradiance the expansion followed up the end of the laser heating the measured temperature. However, the expansion did not return to its original value. This may either be an immediate effect of the irradiation or an insufficient correction of the animal movements. At the highest irradiance the

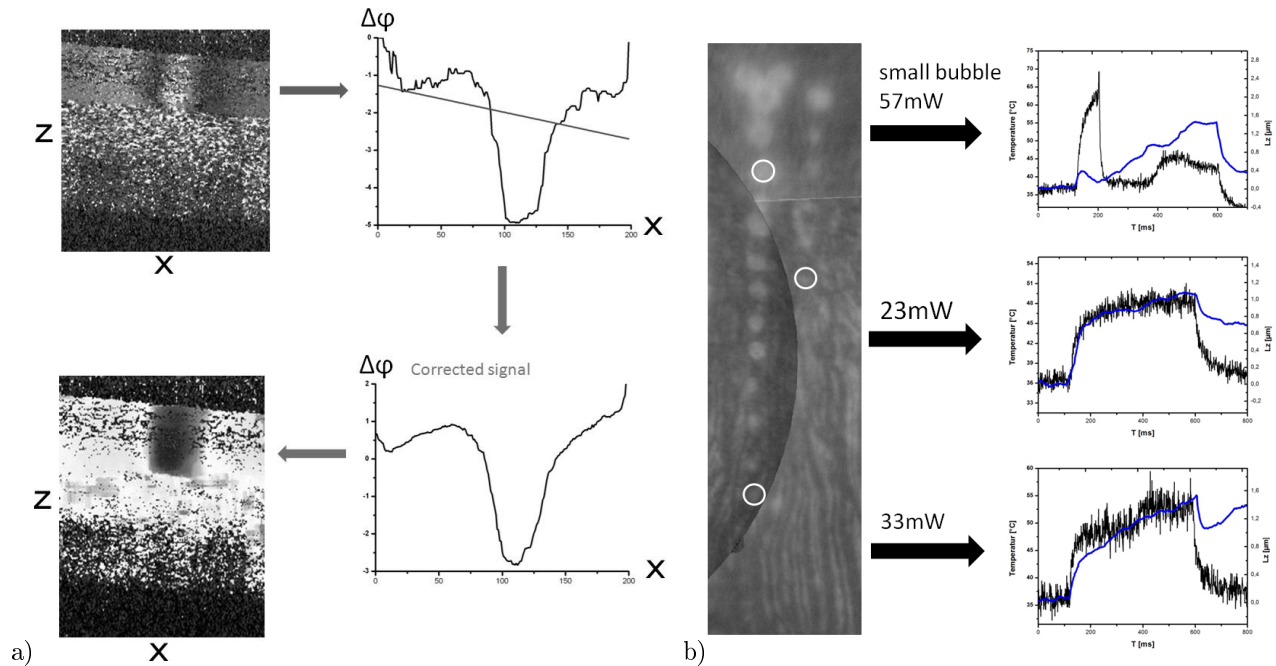


Figure 5. a) The principle of motion correction. b) First in-vivo measurements in rabbit eyes. Left the fluorescence angiogram after irradiation is shown, right see the temperature and expansion curves ΔT and Δz for three different radiant fluxes. Spot diameter was $133\mu\text{m}$

expansions as well as the temperature curve deviate from the expected shape. This was probably caused by a bubble formation in the retina due to excessive heating.

4. CONCLUSION

High speed OCT with A-scan rates of 200 kHz is fast enough to follow on-line the tissue changes during photocoagulation. The whitening of the tissue which is usually observed during photocoagulation was seen time- and spatially resolved during and after the irradiation as an increase of the OCT signal. Though OCT B-Scans seems to have a similar sensitivity as fundus images of the retina in visualizing the coagulation effects, they show the extend of increased scattering also depth resolved and make distortions of the retina due to tissue coagulation visible. A more sensitive marker for the onset of tissue changes are phase changes of the back scattered light which can be visualized by Doppler-OCT. Subthreshold lesions are readily visualized. In conclusion, phase-sensitive OCT can measure temperature increases and thermally induced irreversible tissue changes. The investigation of the mechanisms of photocoagulation by OCT may lead to new treatment protocols for retinal photocoagulation. OCT may also be used as a new tool for a dosimetry of photocoagulation.

5. ACKNOWLEDGMENTS

This project was funded by TANDEM (Center for Technology and Engineering in Medicine) of University and Polytechnicum in Lübeck and the Ministry of Economics and Science in Schleswig-Holstein. Thank to all people of the Thorlabs GmbH in Lübeck, especially Peter Koch and Dierck Hillmann, for excellent technical support.

REFERENCES

1. S. Sivaprasad, M. Elagouz, D. McHugh, O. Shona, and G. Dorin, "Micropulsed diode laser therapy: evolution and clinical applications," *Surv Ophthalmol* **55**(6), pp. 516–30, 2010.
2. J. Roeder, S. H. Liew, C. Klatt, H. Elsner, E. Poerksen, J. Hillenkamp, R. Brinkmann, and R. Birngruber, "Selective retina therapy (srt) for clinically significant diabetic macular edema," *Graefes Arch Clin Exp Ophthalmol* **248**(9), pp. 1263–72, 2010.

3. J. Roider, R. Brinkmann, C. Wirbelauer, H. Laqua, and R. Birngruber, "Subthreshold (retinal pigment epithelium) photocoagulation in macular diseases: a pilot study," *Br J Ophthalmol* **84**(1), pp. 40–7, 2000.
4. G. Schuele, G. Hüttmann, and R. Brinkmann, "Noninvasive temperature measurements during laser irradiation of the retina with optoacoustic techniques," in *Ophthalmic Technologies XII*, F. Manns, P. G. Soederberg, and A. Ho, eds., *Proceedings SPIE* **4611**, pp. 64–71, SPIE, 2002.
5. R. Brinkmann, J. Roider, and R. Birngruber, "Selective retina therapy (srt): a review on methods, techniques, preclinical and first clinical results," *Bull Soc Belge Ophthalmol* (302), pp. 51–69, 2006.
6. K. Schlott, J. Stalljohann, B. Weber, J. Kandulla, K. Herrmann, R. Birngruber, and R. Brinkmann, "Optoacoustic online temperature determination during retinal laser photocoagulation," *Therapeutic Laser Applications and Laser-Tissue Interactions III* **6632**(1), p. 66321B, SPIE, 2007.
7. J. Kandulla, H. Elsner, R. Birngruber, and R. Brinkmann, "Noninvasive optoacoustic online retinal temperature determination during continuous-wave laser irradiation.," *J Biomed Opt* **11**(4), p. 041111, 2006.
8. C. Framme, A. Walter, P. Prahs, R. Regler, D. Theisen-Kunde, C. Alt, and R. Brinkmann, "Structural changes of the retina after conventional laser photocoagulation and selective retina treatment (srt) in spectral domain oct," *Curr Eye Res* **34**(7), pp. 568–79, 2009.
9. B. J. Vakoc, G. J. Tearney, and B. E. Bouma, "Real-time microscopic visualization of tissue response to laser thermal therapy," *J Biomed Opt* **12**(2), p. 020501, 2007.
10. G. Schüle, G. Hüttmann, C. Framme, J. Roider, and R. Brinkmann, "Noninvasive optoacoustic temperature determination at the fundus of the eye during laser irradiation," *Journal of Biomedical Optics* **9**(1), pp. 173–179, 2004.